Supporting Information For

Fluorogenic naked eye "turn-on" sensing of hypochlorous acid by a Zr-based metal-organic framework

*Soutick Nandi,[ab] Subhrajyoti Ghosh,[a] Mostakim SK,[a] and Shyam Biswas *[a]*

[a] *Department of Chemistry, Indian Institute of Technology Guwahati, Guwahati, 781039 Assam, India.*

[b] *Department of Chemistry, Brainware University, Kolkata, 700125 West Bengal, India.*

** Corresponding author. Tel: 91-3612583309, Fax: 91-3612582349.*

E-mail address: sbiswas@iitg.ac.in.

Materials and Characterization Methods. All the required chemicals were purchased from commercial sources and used without purification, except 2-((dimethylthiocarbamoyl)oxy) terephthalic acid (H_2BDC-DMTCM). Fourier transform infrared (FT-IR) spectra were recorded with a Perkin Elmer Spectrum two FT-IR spectrometer in the range of 440-4000 cm^{-1} with KBr pellet. The below mentioned indications were employed for the characterization of the absorption bands: medium (m), weak (w), broad (br), very strong (vs), strong (s) and shoulder (sh). X-Ray powder diffraction (XRPD) patterns were collected by Rigaku Smartlab X-ray diffractometer with copper Kα (λ = 1.54 Å) as the source recorded with a scan rate of 5°/s between 2θ (5-50°) with 9 kW power. FE-SEM images were captured with a Zeiss (Zemini) scanning electron microscope. Thermogravimetric analyses (TGA) were collected under air atmosphere at a heating rate of 10 °C min^{-1} in a temperature region of 25-800 °C by employing a Netzsch STA-409CD thermal analyzer. Fluorescence emission behavior was recorded by a HORIBA JOBIN YVON Fluoromax-4 spectrofluorometer. The excitation wavelength (λ_{ex}) was 305 nm for all the fluorescence experiments. The nitrogen sorption isotherms were performed employing a Quantachrome Autosorb iQ-MP gas sorption analyzer at -196 °C. Prior to the sorption measurement, degassing of the material was performed at 90 °C for 12 h under dynamic vacuum. A Bruker Avance III 600 spectrometer was utilized for recording ^{1}H-NMR at 400 MHz. The mass spectrum (in ESI mode) was measured with an Agilent 6520 Q-TOF high-resolution mass spectrometer. Fluorescence lifetime measurements were performed by time correlated single-photon counting (TCSPC) method by an Edinburgh Instrument Life-Spec II instrument. The fluorescence decays were analyzed by reconvolution method using the FAST software provided by Edinburgh Instruments.

Preparation of 2-((dimethylthiocarbamoyl)oxy) terephthalic acid (H_2BDC-DMTCM). 2-((dimethylthiocarbamoyl)oxy) terephthalic acid (H_2BDC-DMTCM) was prepared by the hydrolysis of its corresponding dimethyl ester compound (Scheme S1). Dimethyl 2-((dimethylthiocarbamoyl)oxy) terephthalate was prepared by following similar reported procedure, which was adopted for 2,5-bis((dimethylthiocarbamoyl)oxy)terephthalic acid diethyl ester.[1] The hydrolysis of the ester compound was carried out by the following method. In 40 mL of methanol, 1 g (3.5 mmol) of dimethyl 2-((dimethylthiocarbamoyl)oxy) terephthalate was dissolved. Afterward, 14 mL of 1 (N) NaOH was added dropwise. The mixture was kept for 12 h under stirring condition. Then, the solution was filtered and conc. HCl was added to reach pH = 3. Then, the methanol was evaporated and the solution was kept at 4 °C. After 3 h, white precipitate was collected and dried at 60 °C for 12 h in a conventional oven. Yield was 620 mg (2.3 mmol, 65 %). ^{1}H-NMR (400 MHz, DMSO-d_6): δ = 3.35 (s, 6H), 7.98-7.96 (d, 1H), 7.89-7.86 (d, 1H), 7.59 (s, 1H) ppm. ^{13}C NMR (100 MHz, DMSO-d_6): δ = 185.98, 165.99, 165.00, 152.87, 134.90, 131.43, 129.01, 126.43, 125.38, 42.86 ppm. ESI-MS (m/z): 268.0396 for $(M-H)^-$ ion (M = mass of H_2BDC-DMTCM ligand). In Figures S1-S3 the NMR and mass spectra of the H_2BDC-DMTCM ligand are shown.

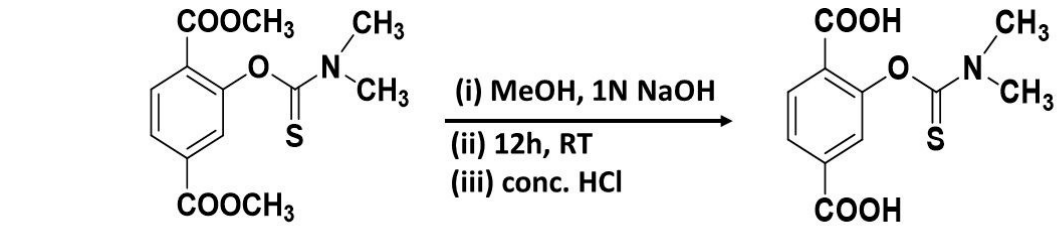

Dimethyl 2-((dimethylthiocarbamoyl)oxy)terephthalate 2-((dimethylthiocarbamoyl)oxy)terephthalic acid

Scheme S1. Scheme for the preparation of 2-((dimethylthiocarbamoyl)oxy) terephthalic acid (H_2BDC-DMTCM).

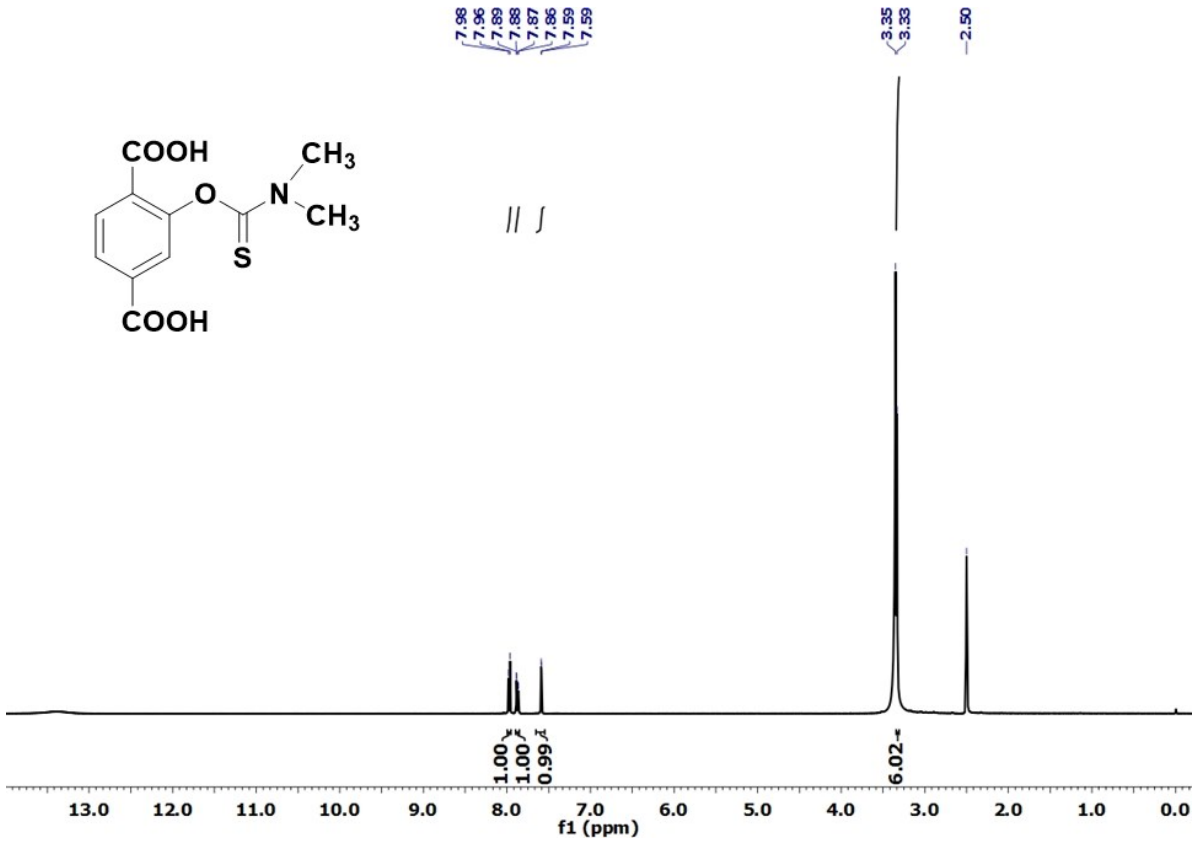

Figure S1. ^{1}H NMR spectrum of 2-((dimethylthiocarbamoyl)oxy) terephthalic acid (H_2BDC-DMTCM) ligand.

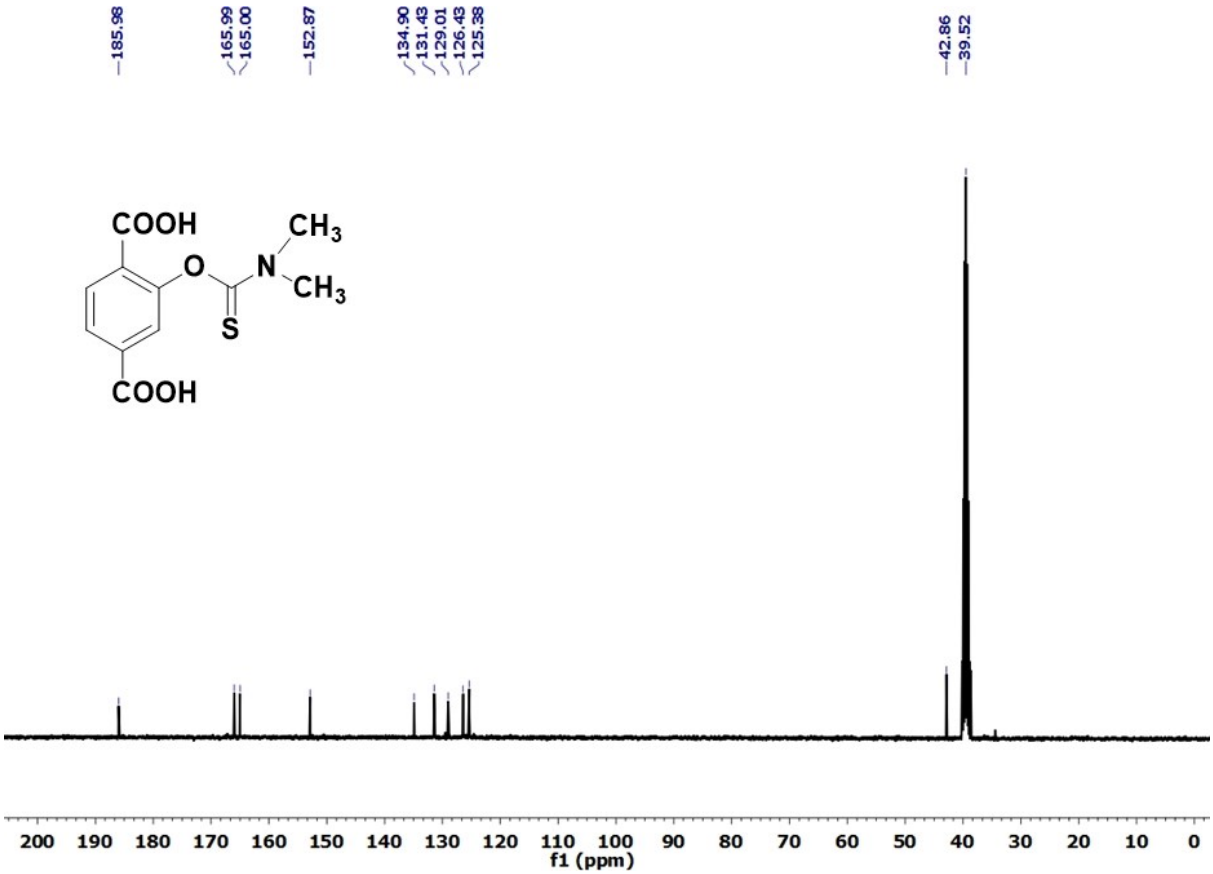

Figure S2. ^{13}C NMR spectrum of 2-((dimethylthiocarbamoyl)oxy) terephthalic acid (H_2BDC-DMTCM) ligand.

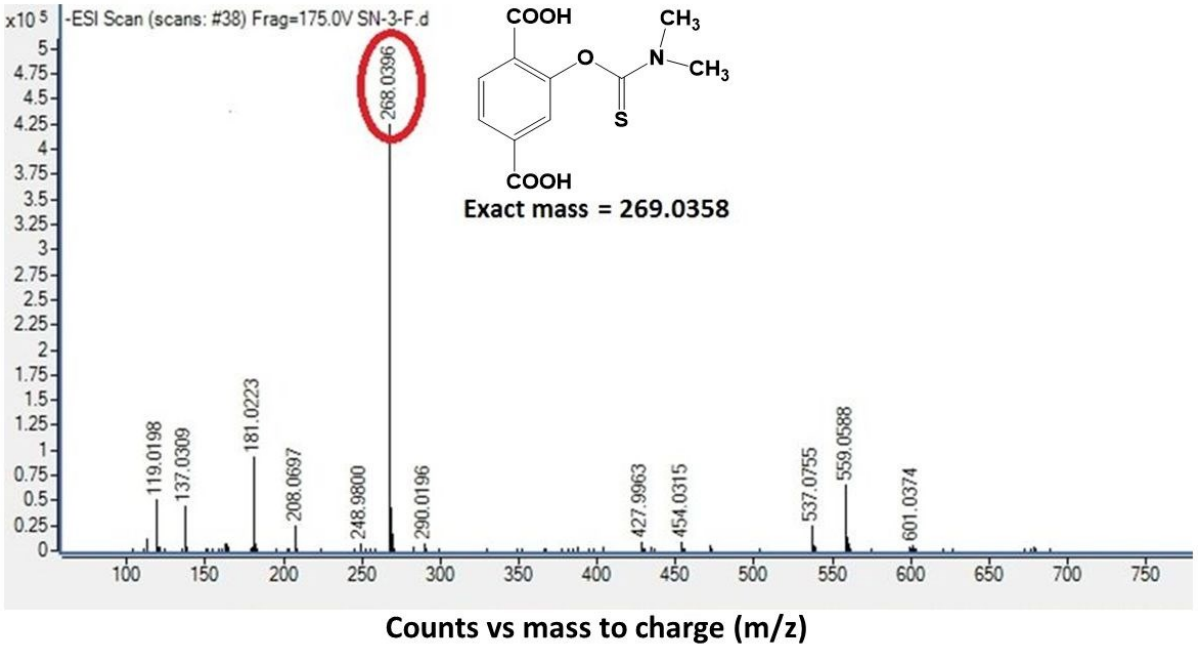

Figure S3. ESI-MS spectrum of 2-((dimethylthiocarbamoyl)oxy) terephthalic acid (H_2BDC-DMTCM) ligand.

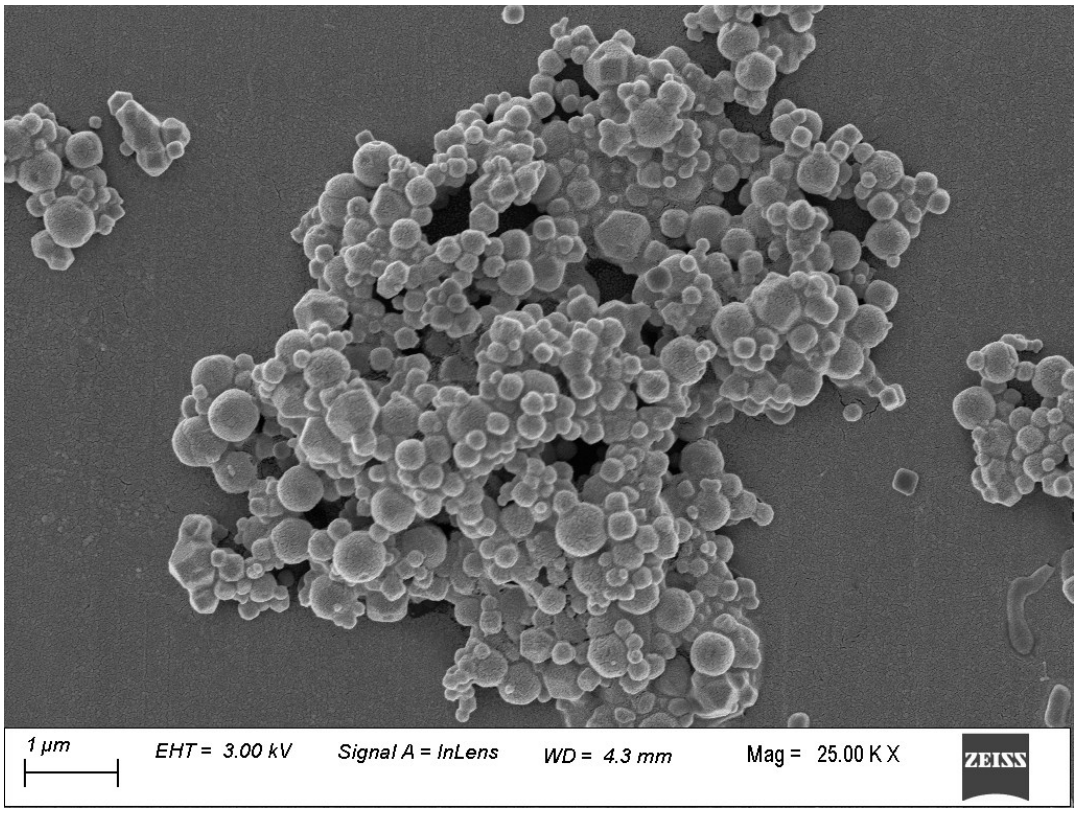

Figure S4. FE-SEM images of **1′**.

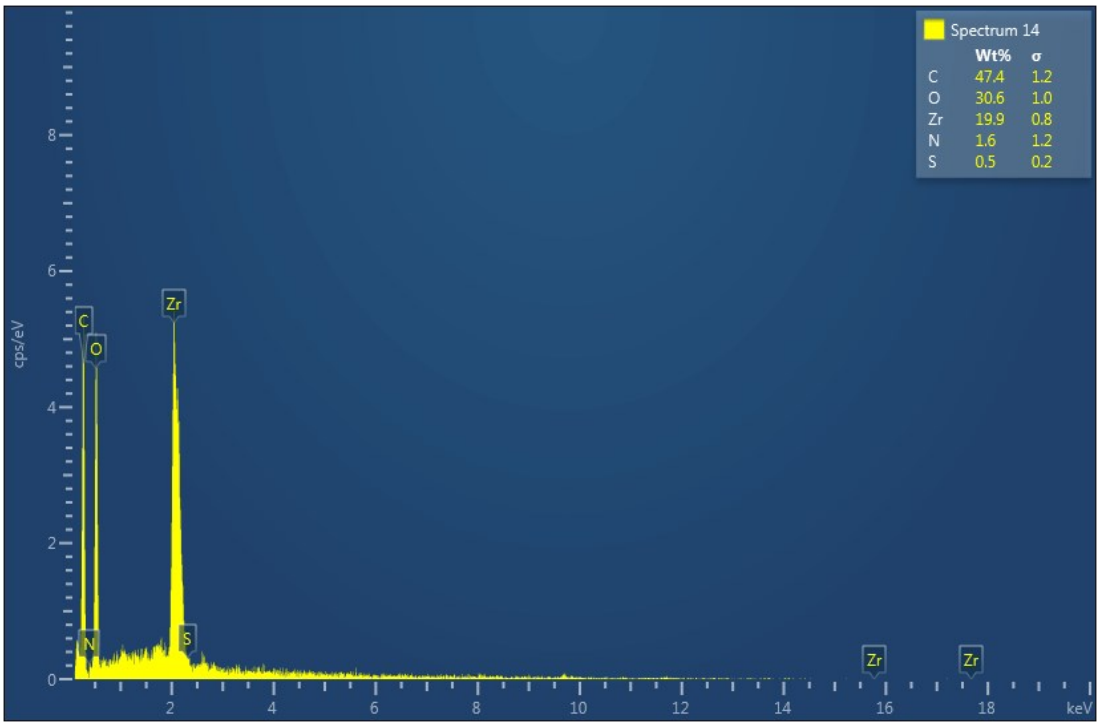

Figure S5. EDX spectrum of **1'**.

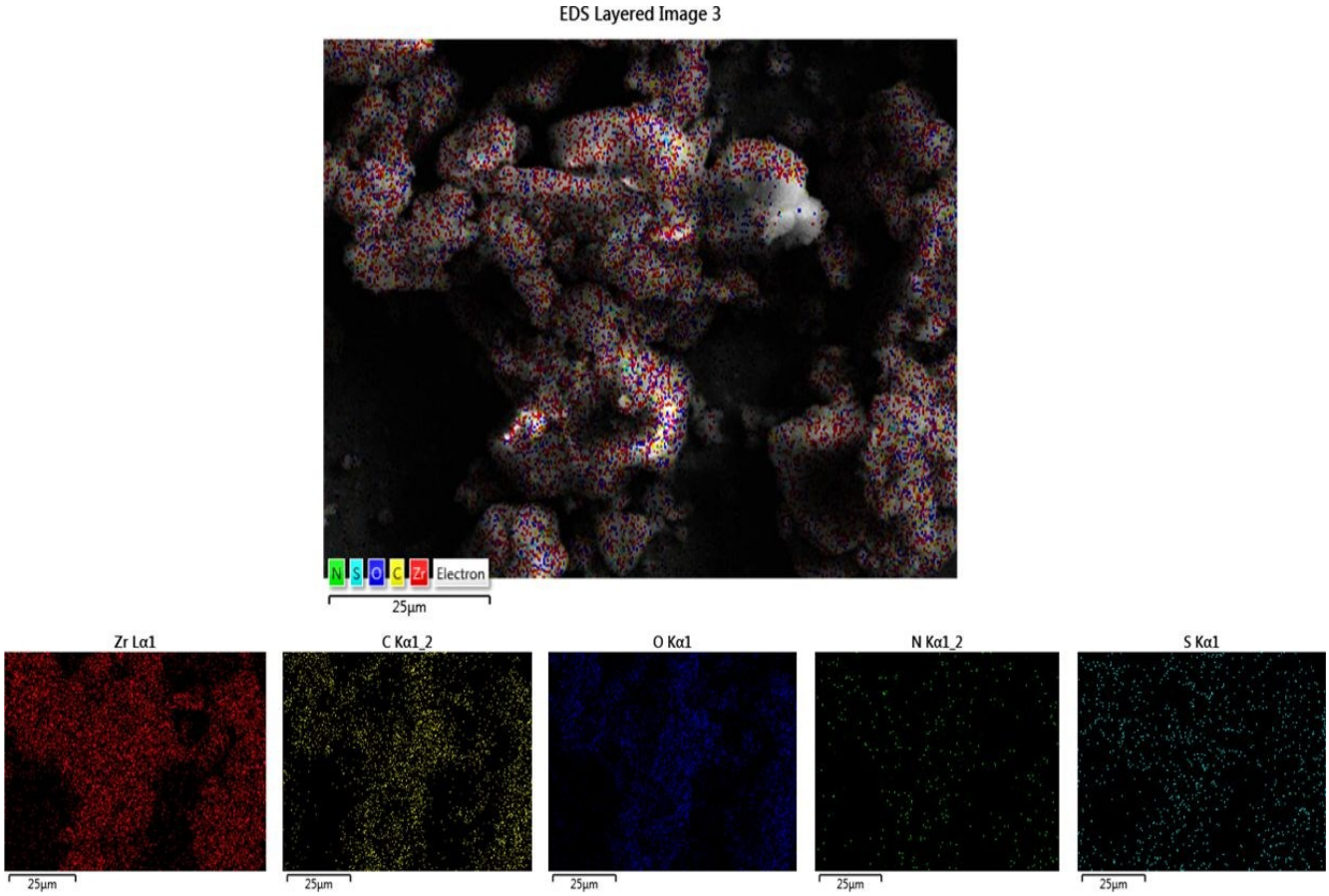

Figure S6. EDX elemental mapping of **1'**.

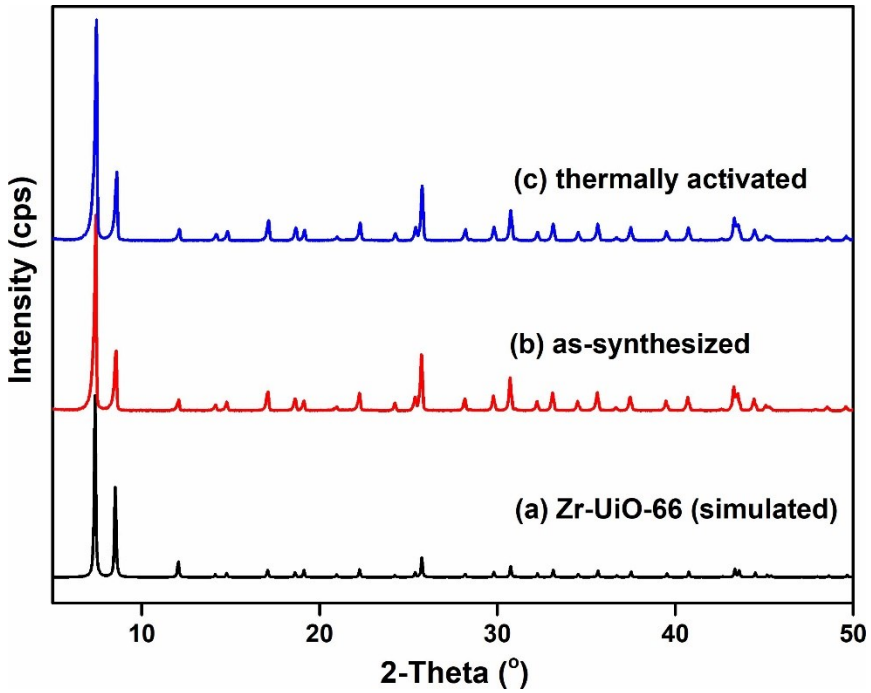

Figure S7. XRPD pattern of the simulated Zr-UiO-66 (black), as-synthesized **1** (red) and thermally activated (blue) **1'**.

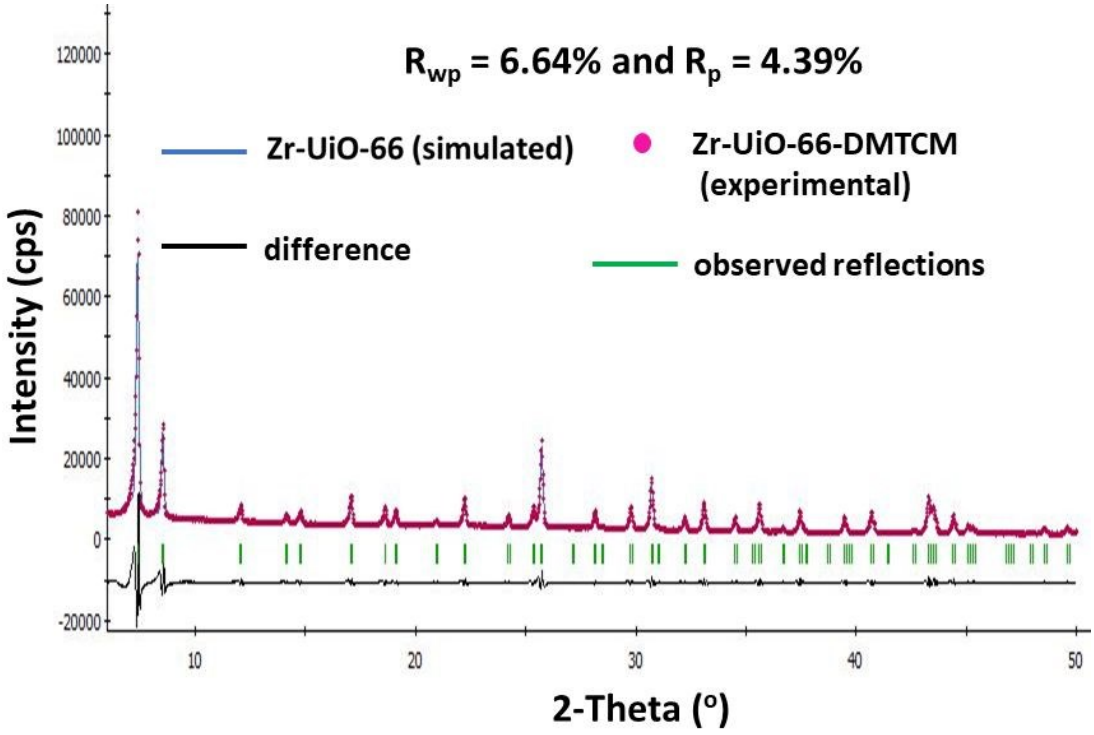

Figure S8. Pawley refinement for the XRPD pattern of as-synthesized **1**. Pink characters and blues lines denote experimental and simulated patterns, respectively. The peak positions and difference plot are shown at the bottom (R_{wp} = 6.64%, R_p = 4.39%).

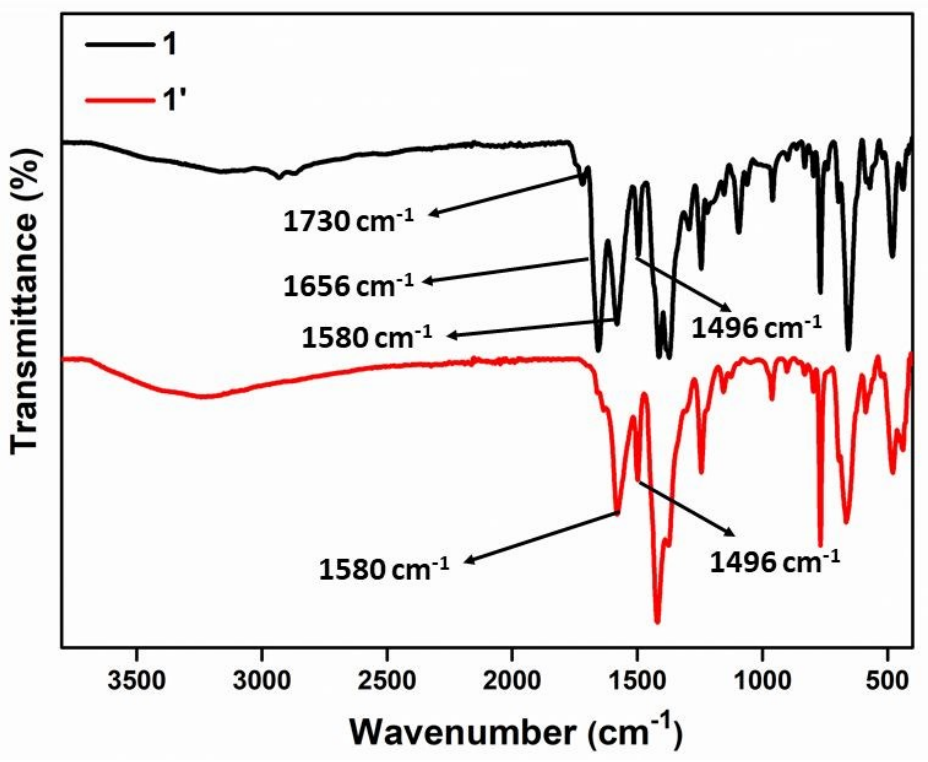

Figure S9. FT-IR spectra of as-synthesized **1** and thermally activated **1′**.

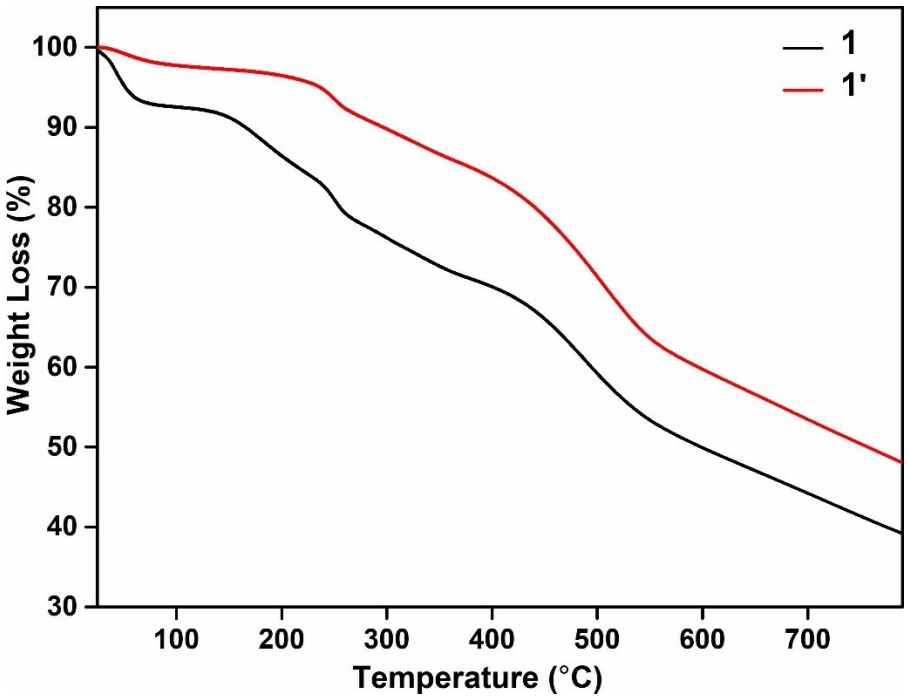

Figure S10. TG curves of as-synthesized and activated material measured in the temperature range of 25-700 °C at a heating rate of 5 ºC min^{-1}.

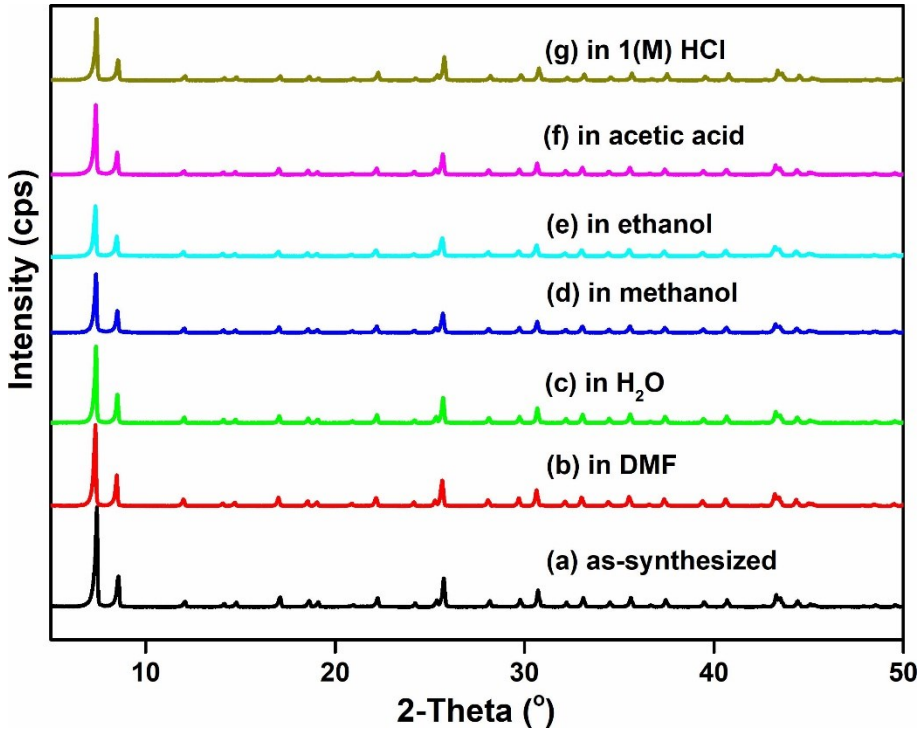

Figure S11. Experimental XRPD patterns of as-synthesized **1** (a), in DMF (b), in H_2O (c), in methanol (d), in ethanol (e) acetic acid (f) and 1(M) HCl (g).

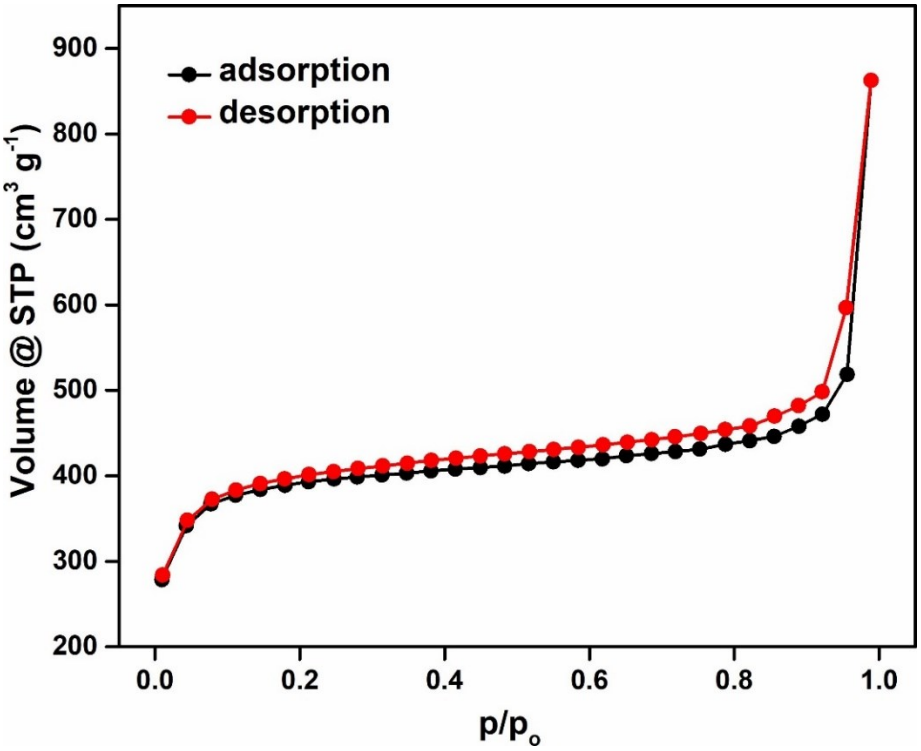

Figure S12. N_2 adsorption (solid black circles) and desorption (solid red circles) isotherms of activated **1'** measured at -196 °C.

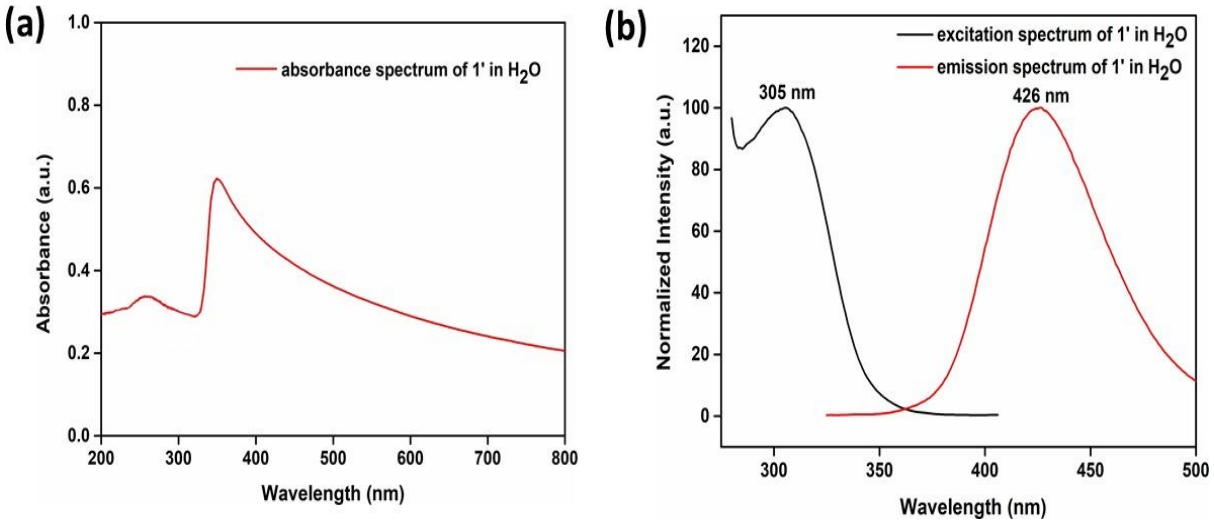

Figure S13. (a) UV-Vis spectrum and (b) fluorescence spectra (excitation and emission) of **1'** in aqueous medium.

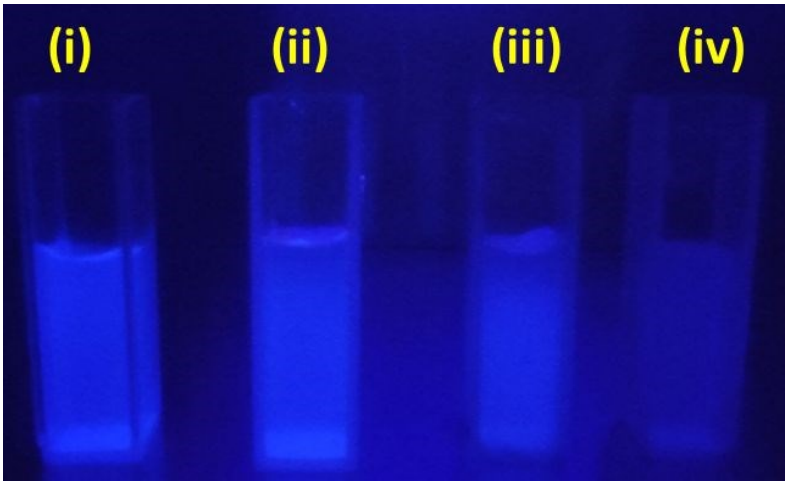

Figure S14. Naked eye detectable color change under UV lamp with the inclusion of (i) 20 μM (ii) 6 μM (iii) 3 μM (iv) 0 μM (blank) concentration of HOCl in aqueous suspension of **1'.**

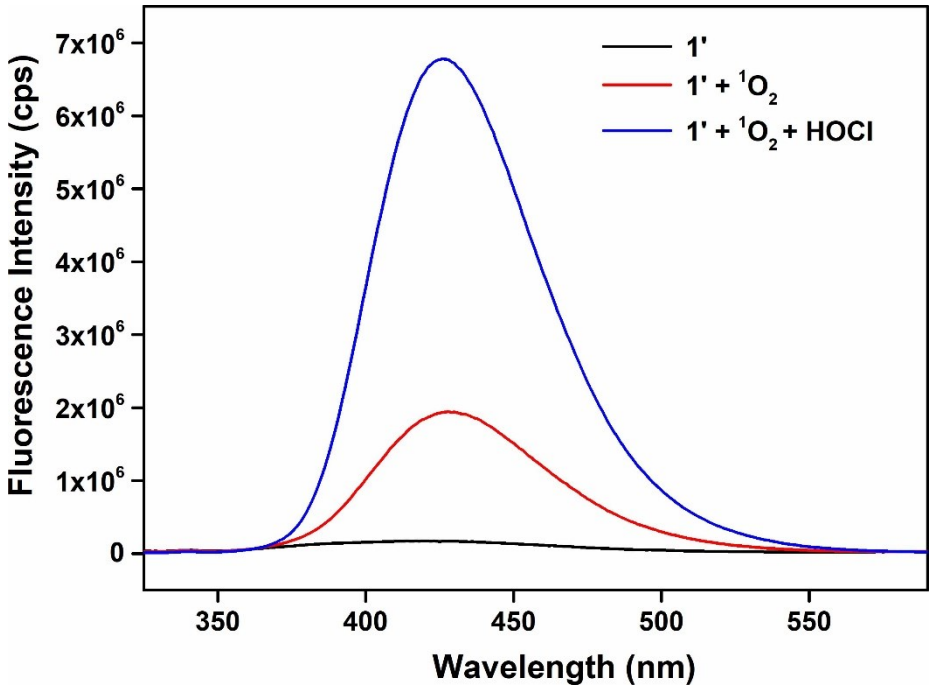

Figure S15. Change in the fluorescence emission intensity of **1′** upon addition of 1 mM HOCl solution (500 μL) in presence of 1 mM $^1O_2$ solution (500 μL).

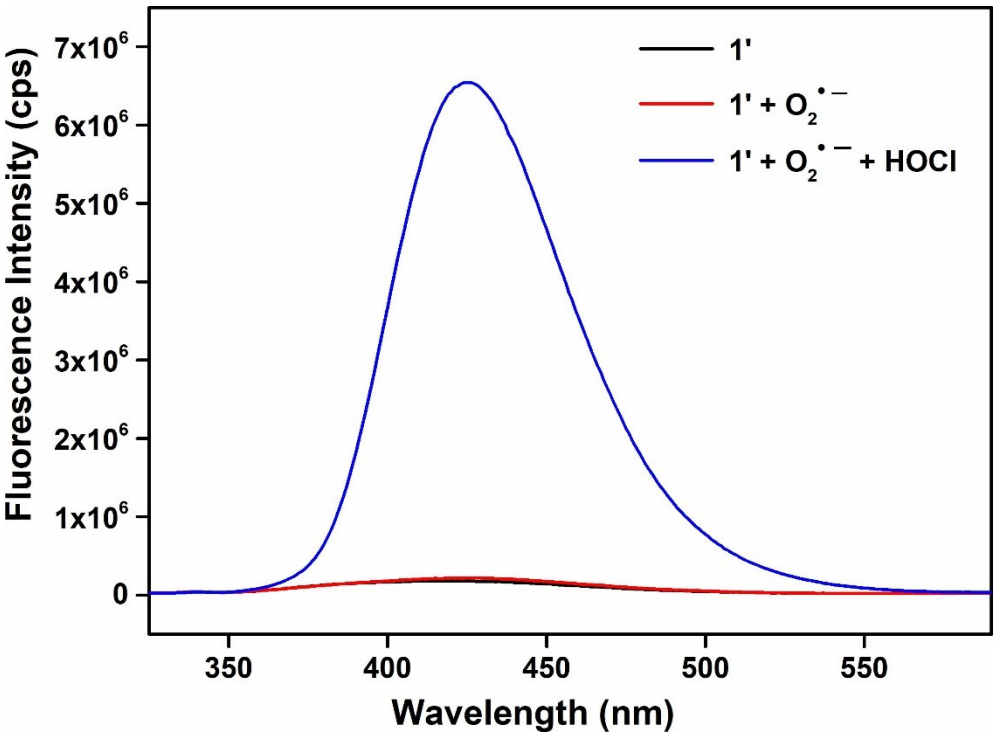

Figure S16. Change in the fluorescence emission intensity of **1′** upon addition of 1 mM HOCl solution (500 µL) in presence of 1 mM $O_2^{\bullet-}$ solution (500 µL).

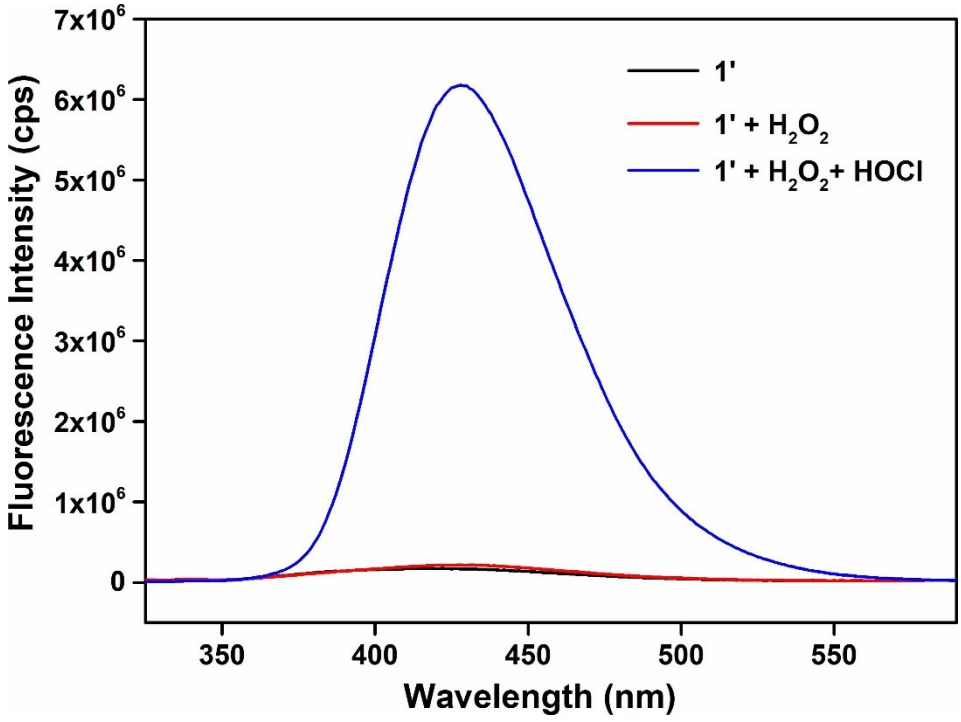

Figure S17. Change in the fluorescence emission intensity of **1′** upon addition of 1 mM HOCl solution (500 µL) in presence of 1 mM H_2O_2 solution (500 µL).

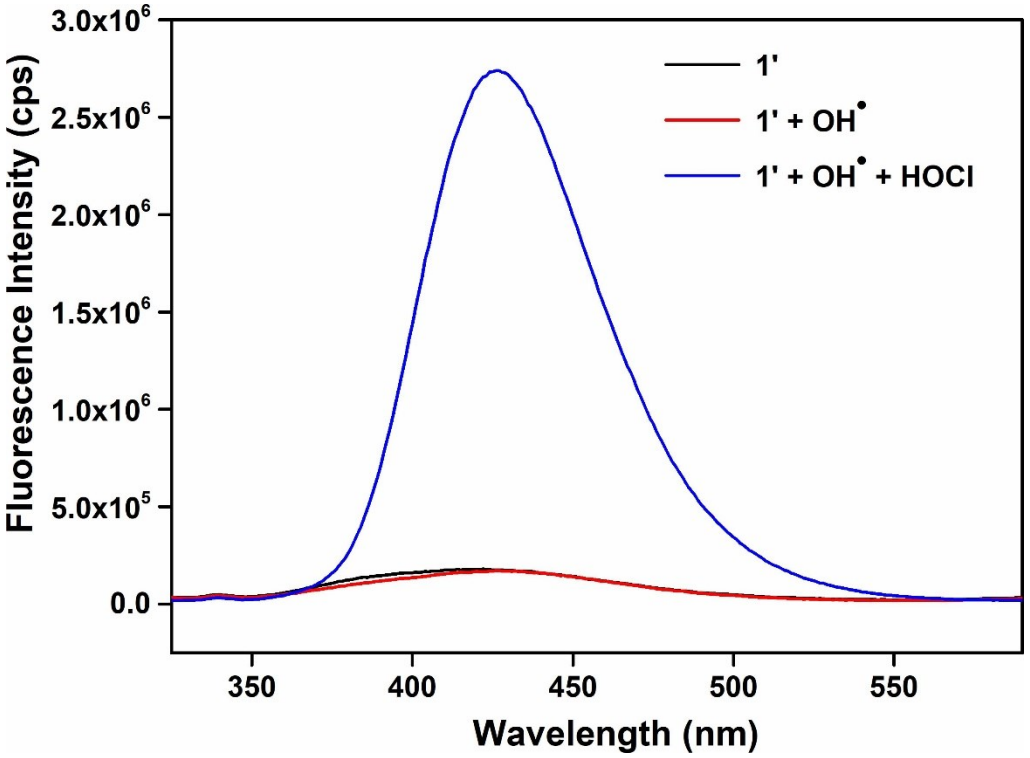

Figure S18. Change in the fluorescence emission intensity of **1′** upon addition of 1 mM HOCl solution (500 µL) in presence of 1 mM OH• solution (500 µL).

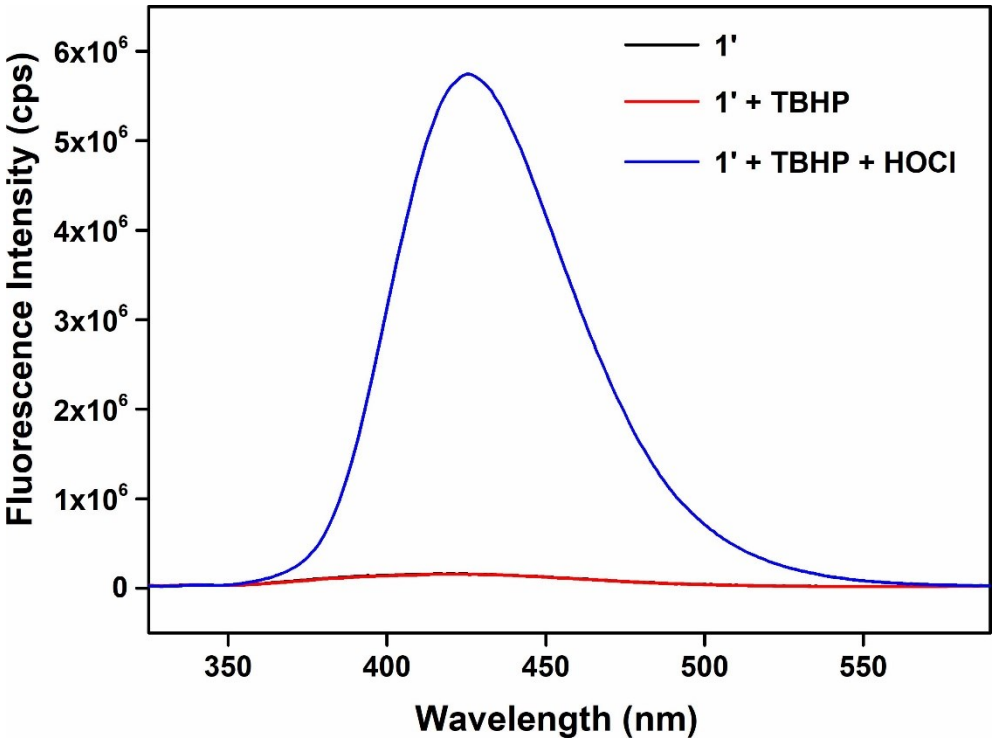

Figure S19. Change in the fluorescence emission intensity of **1′** upon addition of 1 mM HOCl solution (500 µL) in presence of 1 mM TBHP solution (500 µL).

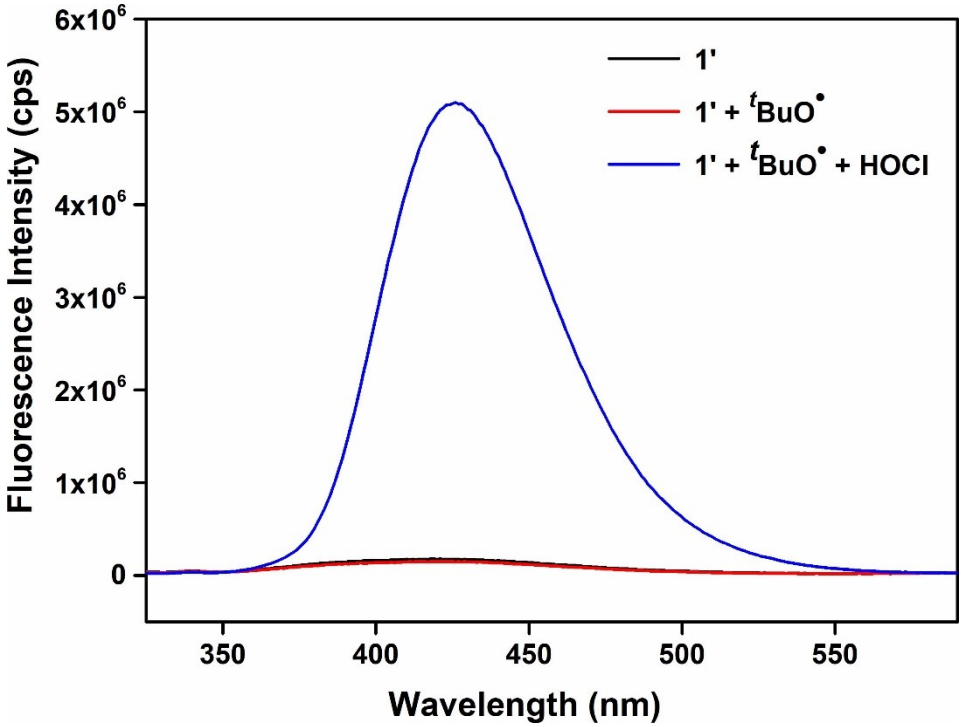

Figure S20. Change in the fluorescence emission intensity of **1′** upon addition of 1 mM HOCl solution (500 µL) in presence of 1 mM ^{t}BuO$^{\bullet}$ solution (500 µL).

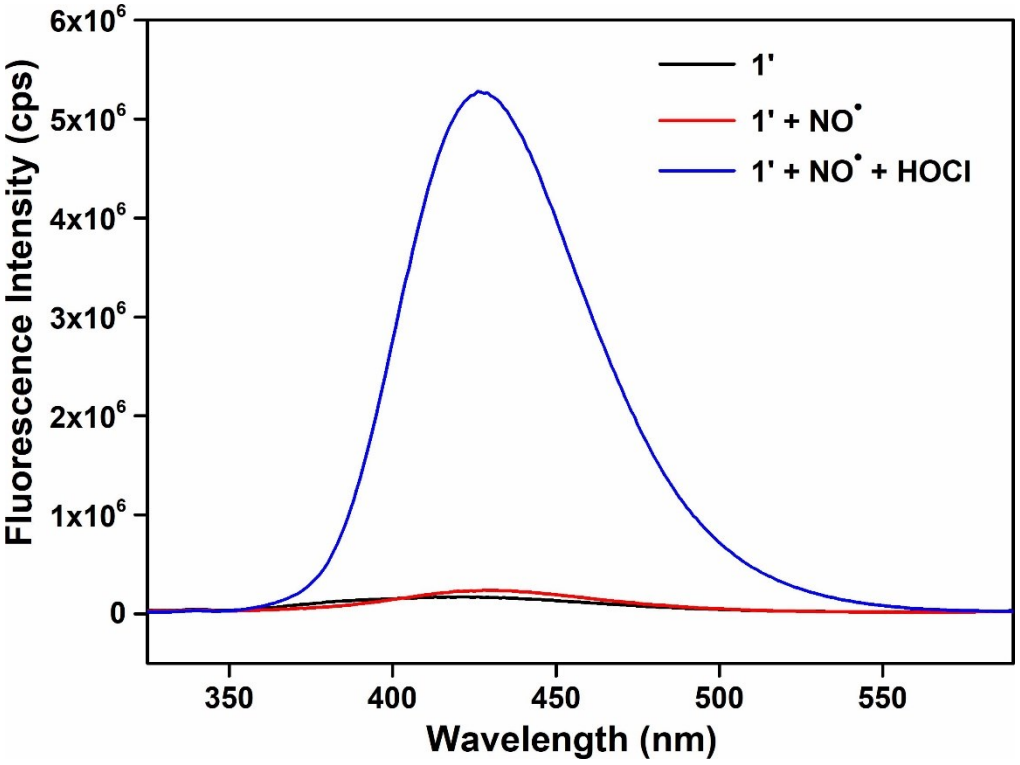

Figure S21. Change in the fluorescence emission intensity of **1′** upon addition of 1 mM HOCl solution (500 µL) in presence of 1 mM NO$^{\bullet}$ solution (500 µL).

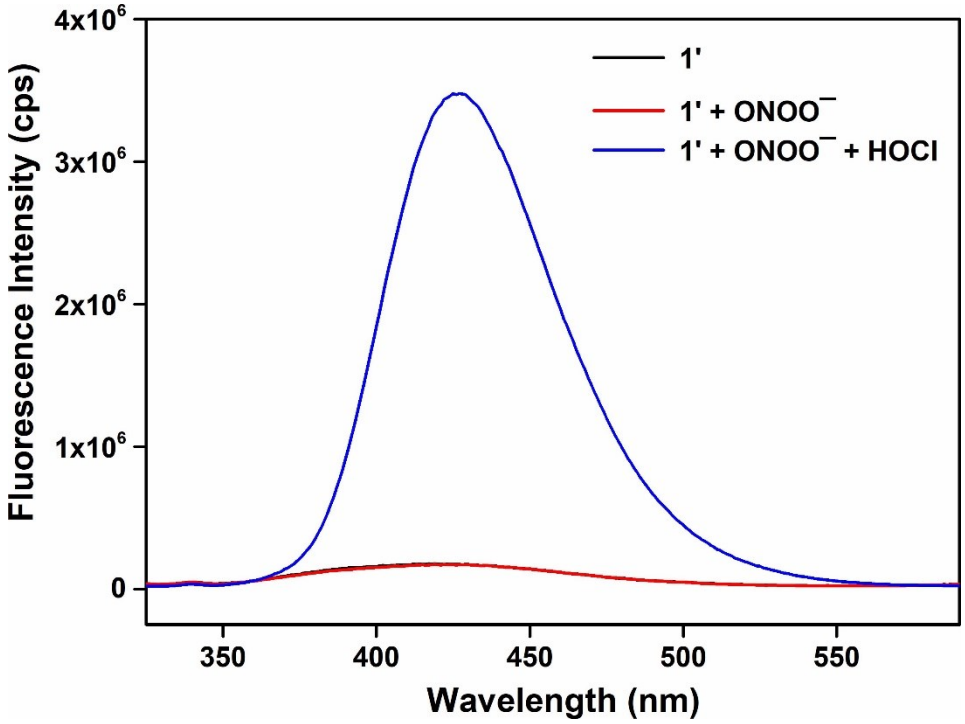

Figure S22. Change in the fluorescence emission intensity of **1′** upon addition of 1 mM HOCl solution (500 μL) in presence of 1 mM $ONOO^-$ solution (500 μL).

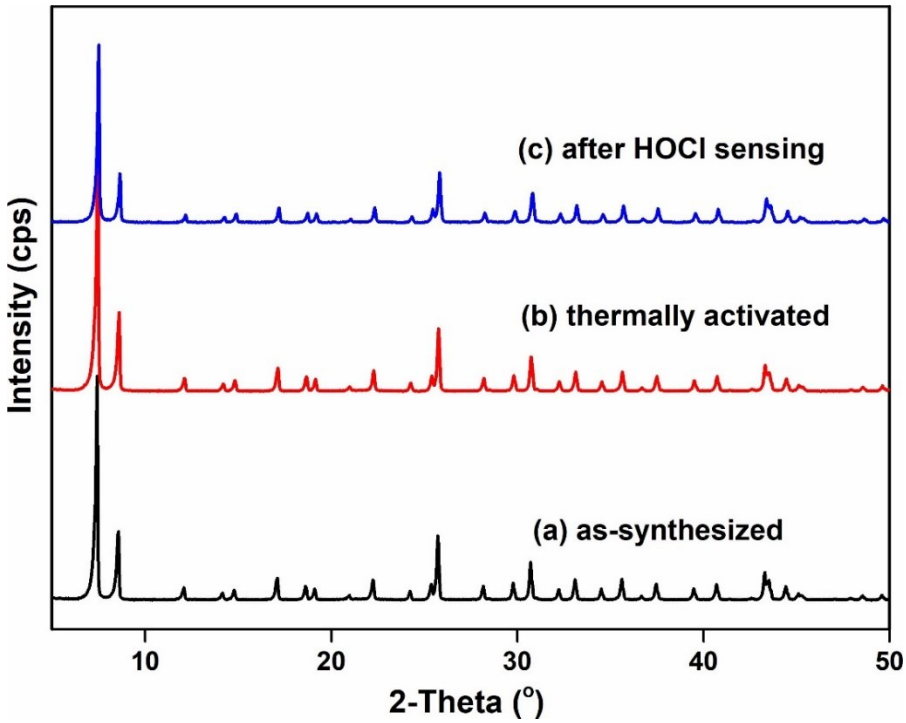

Figure S23. XRPD patterns of **1** in different forms: as-synthesized (a), thermally activated (b) and after HOCl sensing (c).

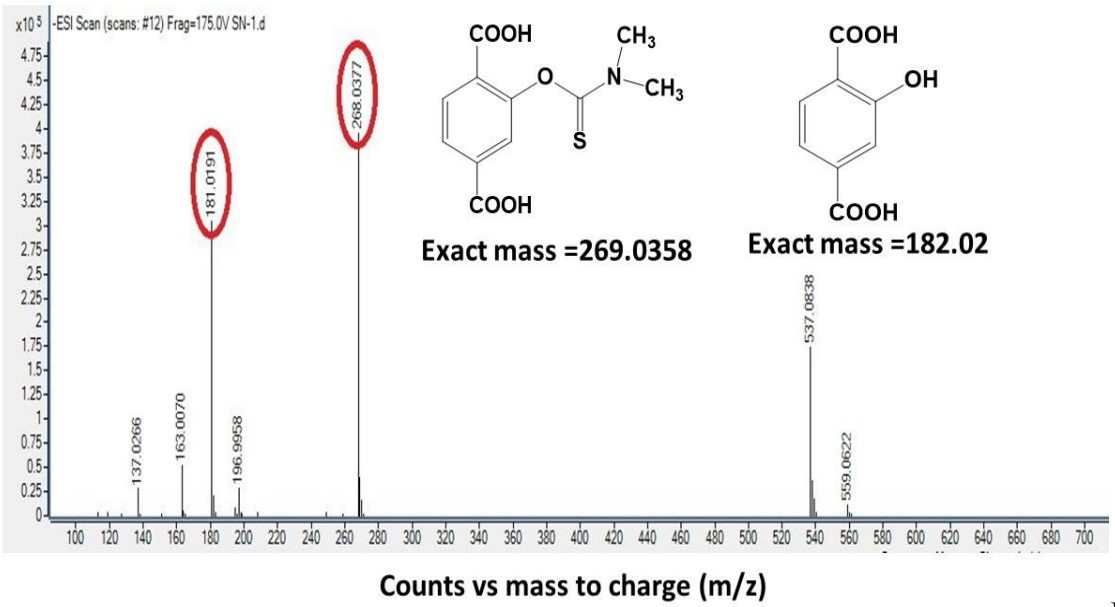

Figure S24. ESI-MS spectrum of HOCl treated H_2BDC-DMTCM in MeOH. The spectrum shows m/z (negative ion mode) peaks at 268.0377 and 181.0191, which correspond to $(M-H)^-$ ion of H_2BDC-DMTCM and HOCl mediated product (i.e. H_2BDC-OH).

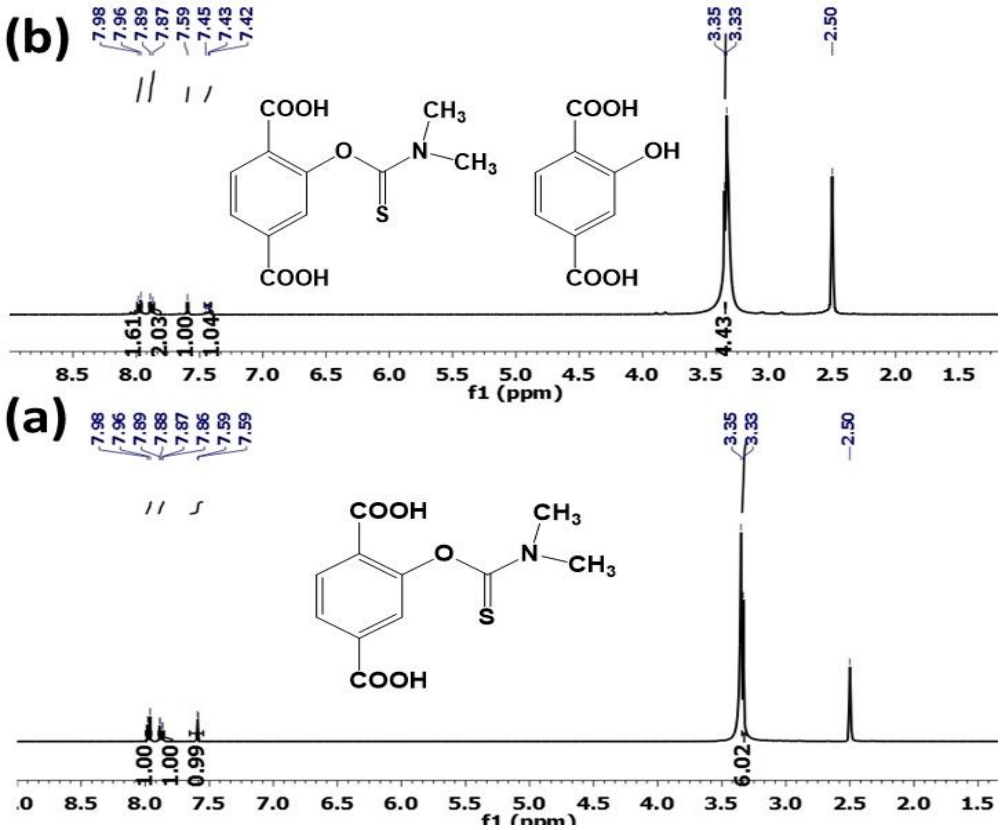

Figure S25. ^{1}H NMR spectrum of (a) H_2BDC-DMTCM ligand and (b) HOCl-treated H_2BDC-DMTCM ligand in DMSO-d_6. New proton signals at 7.88 ppm and 7.45-7.42 ppm signifies the formation of H_2BDC-OH after treatment with HOCl solution.

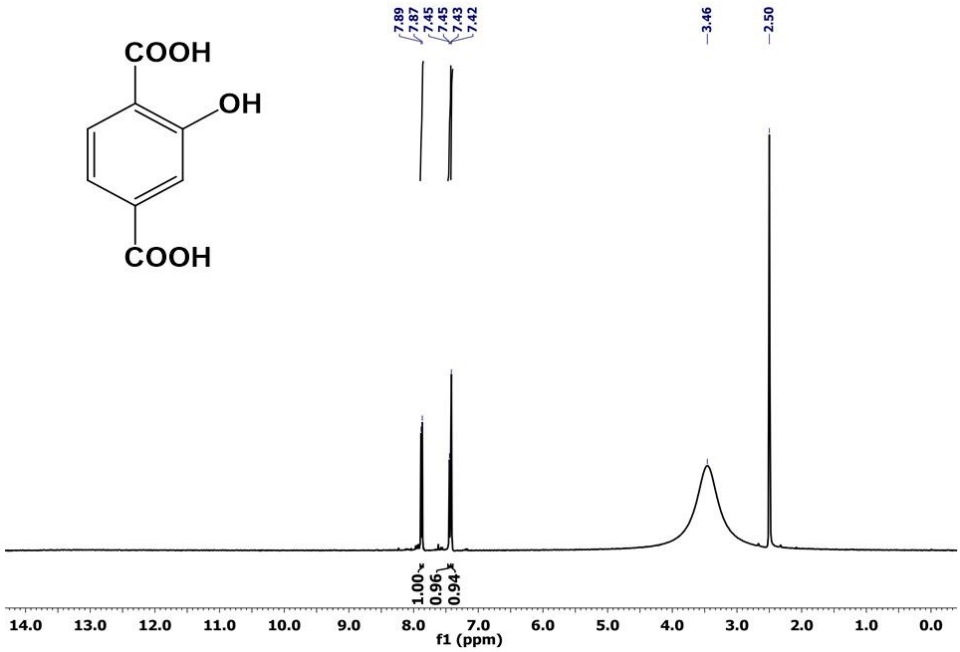

Figure S26. ^{1}H NMR spectrum spectrum of 2-hydroxy terephthalic acid (H_2BDC-OH) ligand.

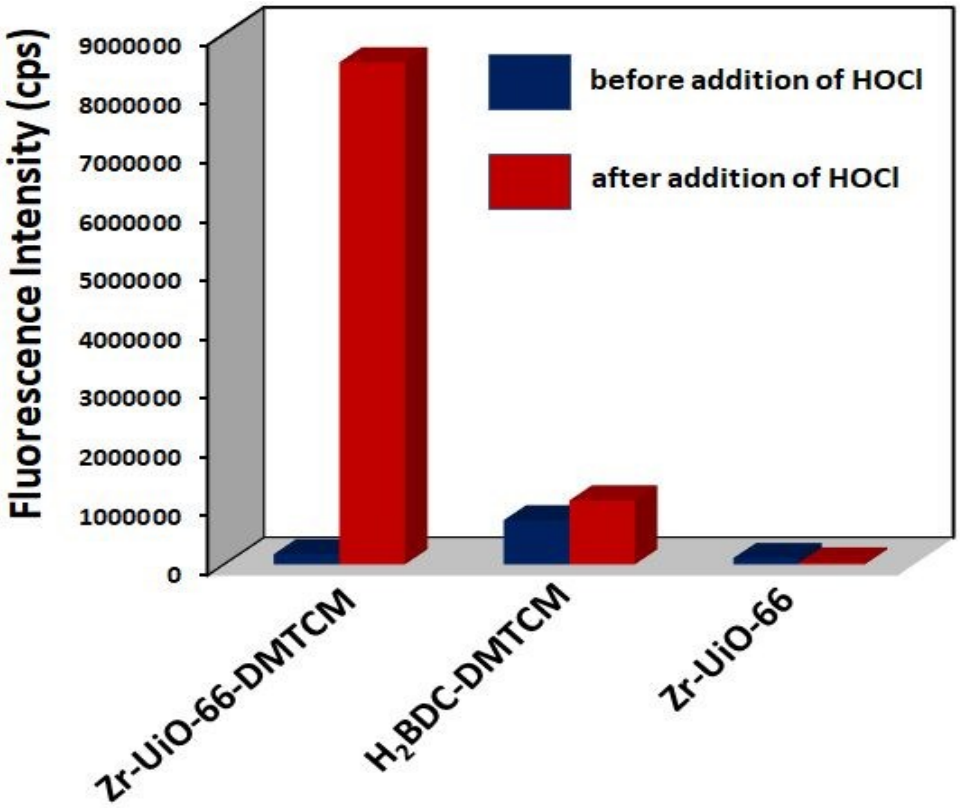

Figure S27. Relative fluorescence response of **1′**, H_2BDC-DMTCM and unfunctionalized Zr-UiO-66 towards 1 mM HOCl (500 µL) in aqueous medium.

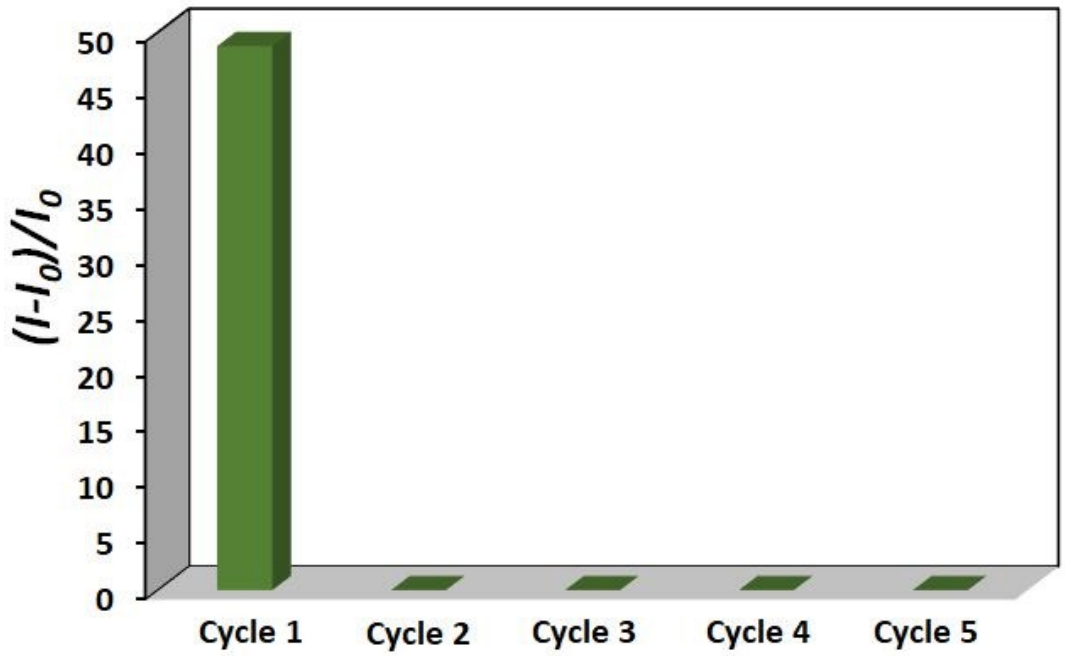

Figure S28. Recyclability test for the fluorescence turn-on response of **1′** towards HOCl solution.

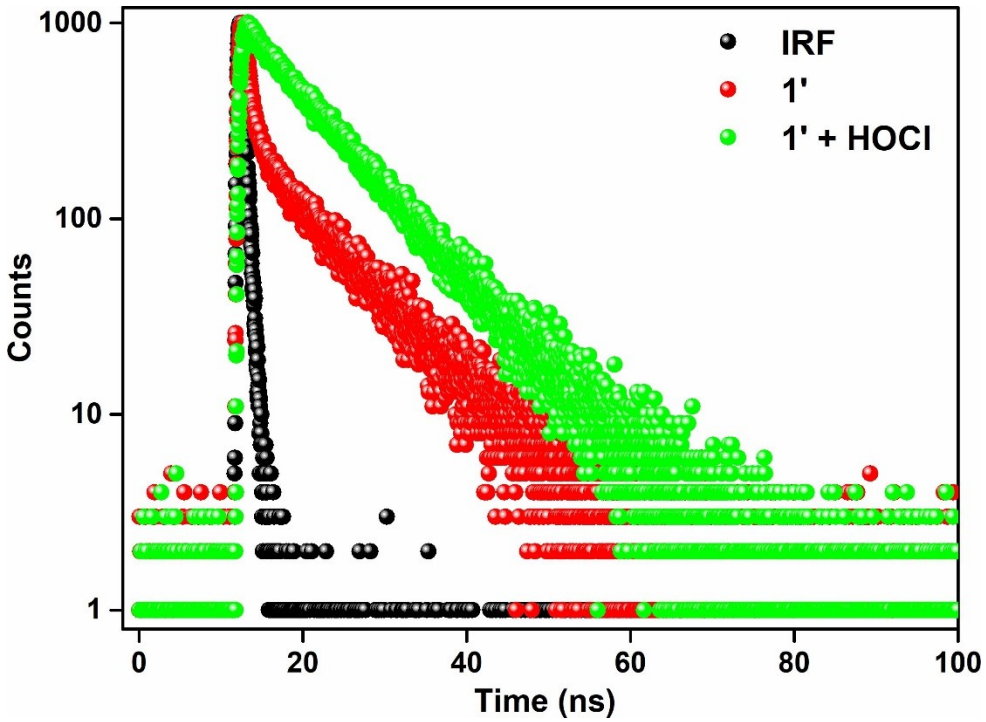

Figure S29. Lifetime decay profiles of aqueous suspension of **1′** in absence and presence of HOCl solution (λ_{ex} = 290 nm, monitored at 425 nm).

Table S1. Comparison of the sensing performance of various sensors of HOCl.

Sl. No.	Sensor	Type of Material	Sensing Medium	Mode of Detection	Detection Limit	Response Time	Ref.
1	Zr-UiO-66-DMTCM)) (**1**)	MOF	Water	Fluorescence "Turn-on"	1.22 μM	Second	this work
2	UiO-68-ol	MOF	PBS buffer	Fluorescence "Turn-off"	10^{-7} M	Second	2
3	Eu-BDC-NH_2 /DPA	MOF	-	Ratiometric	37 nM	Second	3
4	Flu-1	Organic molecule	DMSO–H_2O	Fluorescence "Turn-on"	-	Second	4
5	Naph-1 and Naph-2	Organic molecule	PBS buffer	Fluorescence "Turn-on"	37 nM and 8.2 nM	1 min	5
6	rTP-HOCl 1	Organic molecule	PBS buffer	Ratiometric	34.8 nM	Second	6
7	HySOx	Organic molecule	Sodium phosphate buffer containing 20% DMF	Fluorescence "Turn-on"	-	Second	7
8	Compound **1**	Organic molecule	0.1M potassium phosphate buffer pH 9.0/DMF (v/v, 1:4)	Fluorescence "Turn-off"	-	3 min	8
9	FBS	Organic molecule	KH_2PO4 buffer (50 mM, pH 7.4)	Fluorescence "Turn-on"	0.2 μM	-	9
10	TP-HOCl 1	Organic molecule	PBS buffer	Fluorescence "Turn-on"	16.6 nM	Second	10
11	PMOPP	Organic	PBS solution	Fluorescence "Turn-	0.8 μM	-	11

		molecule	(pH=7.4, 0.01 M)	off"			
12	L1	Organic molecule	PBS buffer	Fluorescence "Turn-off"	0.674 μM	2.5 min	12
13	$[Ir(ppy)_2(L_1)](PF_6)$(1)	Metal complexes	DMF–HEPES (50 mM, pH = 7.2, v/v = 4 : 1)	Fluorescence "Turn-on"	1 ppm	-	13
14	PDA@ERGO/GC	Electrode	Water	Electrochemical	44 nM	-	14
15	BDD	Electrode	Water	Electrochemical	8.3 μM	-	15
16	$AgCl/Ag_2O$ films	Electrode	Water	Electrochemical	2 ppm	60 s	16
17	CuO-NPs@MWCNT	Nanocomposite	PBS	Electrochemical	0.7 μM	-	17
18	Poly MnTAPP-nano Au GCE	Electrode	$NaOH/H_2O$	Electrochemical	24 μM	-	18
19	*o*-tolidinium dichloride	Organic molecule	Buffer solution	Spectrophotometric	0.08 ppm	-	19
20	Acetylcholine esterase	Enzyme	Water	Potentiometric	0.01 mM	20 min	20
21	Styrene	Organic molecule	Water	Gas chromatography/mass spectrometry	0.1 μM	-	21
22	Poly(luminol) reagent film	Thin film	Water	Chemiluminescence	0.5 μM	-	22
23	Glassy carbon electrode	Electrode	Soil	Chronoamperometric	-	2 s	23

Table S2. Unit cell parameters of the as-synthesized Zr-UiO-66-DMTCM MOF (**1′**). The obtained values are compared with the previously reported Zr-UiO-66 MOFs.

Compound Name	Zr-UiO-66-DMTCM MOF (**1′**)	Zr-UiO-66 MOF (reported)[24]	Zr-UiO-66-$(OCOCH_3)_2$ MOF (reported)[25]	Zr-UiO-66-NH-CH_2-Py MOF (reported)[26]	Zr-UiO-66-1-(aminomethyl) naphthalen-2-ol (reported)[27]
Crystal System	cubic	cubic	cubic	cubic	cubic
a = b = c (Å)	20.8029 (7)	20.7004 (2)	20.840(7)	20.755(3)	20.786(3)
α = β= γ (°)	90	90	90	90	90
V ($Å^3$)	9002.5 (5)	8870.3(2)	9051.7(5)	8940.3(21)	8981.1(19)

Table S3. Calculation of detection limit for HOCl detection by **1′**.

Number of Run (n)	Fluorescence Intensities at 425 nm before addition of HOCl	Standard Deviation (σ)	Slope (k) (mM^{-1})	Detection Limit ($3\sigma/k$) (mM)
1	181704.19511	894.18	2.20×10^6	1.22×10^{-3} (1.22 μM)
2	182786.60313			
3	184394.7706			
4	183999.40793			
5	182430.22763			
6	182813.79891			
7	182277.7180			
8	181902.77905			

Table S4. Fluorescence lifetimes of aqueous suspension of **1′** before and after the addition of HOCl solution (λ_{ex} = 290 nm, pulsed diode laser).

Volume of 1 mM HOCl solution added (μL)	a_1	a_2	τ_1 (ns)	τ_2 (ns)	$\langle\tau\rangle$* (ns)	χ^2
0	0.46	0.54	0.55	8.43	4.80	1.01
500	0.04	0.96	1.07	9.04	8.72	1.02

* $\langle\tau\rangle = a_1\tau_1 + a_2\tau_2$

References:

1. P.-T. Skowron, M. Dumartin, E. Jeamet, F. Perret, C. Gourlaouen, A. Baudouin, B. Fenet, J.-V. Naubron, F.Fotiadu, L. Vial and J. Leclaire, *J. Org. Chem.*, 2016, **81**, 654-661.
2. Y.-A. Li, S. Yang, Q.-Y. Li, J.-P. Ma, S. Zhang and Y.-B. Dong, *Inorg. Chem.2017, 56,* , 2017, **56**, 13241-13248.
3. Y.-Q. Sun, Y. Cheng and X.-B. Yin, *Anal. Chem.*, 2021, doi.org/10.1021/acs.analchem.1020c05040.
4. X. Cheng, H. Jia, T. Long, J. Feng, J. Qin and Z. Li, *Chem. Commun.*, 2011, **47**, 11978–11980.
5. Y. Jiang, G. Zheng, Q. Duan, L. Yang, J. Zhang, H. Zhang, J. He, H. Sun and D. Ho, *Chem. Commun.*, 2018, **54**, 7967-7970.
6. Y. W. Jun, S. Sarkar, S. Singha, Y. J. Reo, H. R. Kim, J.-J. Kim, Y.-T. Chang and K. H. Ahn, *Chem. Commun.*, 2017, **53**, 10800-10803.
7. S. Kenmoku, Y. Urano, H. Kojima and T. Nagano, *J. Am. Chem. Soc.*, 2007, **129**, 7313-7318.
8. J. Shi, Q. Li, X. Zhang, M. Peng, J. Qin and Z. Li, *Sens. Actuators, B*, 2010, **145**, 583–587.
9. Q. Xu, K.-A. Lee, S. Lee, K. M. Lee, W.-J. Lee and J. Yoon, *J. Am. Chem. Soc.*, 2013, **135**, 9944-9949.
10. L. Yuan, L. Wang, B. K. Agrawalla, S.-J. Park, H. Zhu, B. Sivaraman, J. Peng, Q.-H. Xu and Y.-T. Chang, *J. Am. Chem. Soc.*, 2015, **137**, 5930–5938.
11. W. Zhang, C. Guo, L. Liu, J. Qin and C. Yang, *Org. Biomol. Chem.*, 2011, **9**, 5560–5563.
12. B. Zhang, X. Yang, R. Zhang, Y. Liu, X. Ren, M. Xian, Y. Ye and Y. Zhao, *Anal. Chem.*, 2017, **89**, 10384-10390.
13. N. Zhao, Y.-H. Wu, R.-M. Wang, L.-X. Shi and Z.-N. Chen, *Analyst*, 136, **2011**, 2277–2282.
14. D. R. Kumar, S. Kesavan, T. T. Nguyen, J. Hwang, C. Lamiel and J.-J. Shim, *Sensors and Actuators B: Chemical*, 2017, **240**, 818-828.
15. M. Murata, T. A. Ivandini, M. Shibata, S. Nomura, A. Fujishima and Y. Einaga, *J. Electroanal. Chem.*, 2008, **612**, 29-36.
16. M. Jović, F. Cortés-Salazar, A. Lesch, V. Amstutz, H. Bi and H. H. Girault, *J. Electroanal. Chem.*, 2015, **756**, 171-178.
17. J. Muñoz, F. Céspedes and M. Baeza, *Microchem. J.*, 2015, **122**, 189-196.
18. S. Thiagarajan, Z.-Y. Wu and S.-M. Chen, *J. Electroanal. Chem.*, 2011, **661**, 322-328.
19. D. J. Leggett, N. H. Chen and D. S. Mahadevappa, *Analyst*, 1982, **107**, 433-441.

20. A. P. Soldatkin, D. V. Gorchkov, C. Martelet and N. J. Renault, *Sens. Actuators B*, 1997, **43**, 99-104.
21. K. Wakigawa, A. Gohda, S. Fukushima, T. Mori, T. Niidome and Y. Katayama, *Talanta*, 2013, **103**, 81-85.
22. M. Szili, I. Kasik, V. Matejec, G. Nagy and B. Kovacs, *Sens. Actuators B*, 2014, **192**, 92-98.
23. L. Kiss, B. Kovacs and G. Nagy, *J. Solid State Electrochem.*, 2015, **19**, 261-267.
24. J. H. Cavka, S. Jakobsen, U. Olsbye, N. Guillou, C. Lamberti, S. Bordiga and K. P. Lillerud, *J. Am. Chem. Soc.*, 2008, **130**, 13850-13851.
25. S. Nandi, M. SK and S. Biswas, *Dalton Trans*, 2020, **49**, 2830-2834.
26. A. Das, N. Anbu, M. SK, A. Dhakshinamoorthy and S. Biswas, *Dalton Trans.*, 2019, **48**, 17371-17380.
27. A. Das, N. Anbu, M. SK, A. Dhakshinamoorthy and S. Biswas, *ChemCatChem*, 2020, **12**, 1789-1798.